Investigation of exciton condensation in nonuniformly deformed germanium using cyclotron resonance and microwave conductivity

A. G. Makarov, A. A. Manenkov, G. N. Mikhaĭlova, and A. S. Seferov

P.N. Lebedev Physics Institute, USSR Academy of Sciences
(Submitted 14 June 1980)
Zh. Eksp. Teor. Fiz. **80**, 638–649 (February 1981)

The microwave conductivity in a zero magnetic field and the cyclotron resonance (CR) were investigated at 9.6 GHz in germanium nonuniformly stressed in the ⟨110⟩ and ⟨111⟩ directions and excited by a pulsed laser ($\lambda = 1.06$ μm). The observed CR line shape revealed an inhomogeneous distribution of the free carriers around electron hole drops. The carrier densities near the EHD surface ($n_{cs} \approx 3.5 \times 10^{12}$ cm^{-3}), the spatial distribution, and the collision frequency are determined from the observed CR line shape. It is shown that the free carriers (FC) and free excitons (FE) are localized in a layer of ~ 60 μm around the EHD and have a Boltzmann density distribution. The kinetics of the EHD was investigated by measuring the microwave conductivity of the FC cloud surrounding the drop. The experimental data are discussed on the basis of an analysis of the kinetic equations for the EHD–FE–FC system. It is established that the pressure gradient in the potential well does not hinder exciton evaporation from the drop, and that this process shortens substantially the EHD lifetime in the $T = 2.8$–4.2 K range. The condensation energy of the FE ($\Phi \approx 1.1$ meV), the work function of the FC ($E_w \simeq 4.6$ meV), and exciton binding energy ($\mathscr{E}_0 \approx 3.5$ meV) are determined. The values of the thermodynamic parameters do not depend on the compression direction in the high-pressure limit ($p \geq 1000$ bar).

PACS numbers: 71.35. + z, 72.20.Jv, 72.80.Cw, 76.40. + b

1. INTRODUCTION

Ever since the first observation of large electron-hole drops (EHD) produced at low temperature in inhomogeneously compressed Ge,[1] many investigations of their physical properties were made and were used to determine many parameters of the EHD (see the review[2]). Nevertheless, many aspect of this problem require further study. This pertains, in particular, to the kinetics of EHD condensation, to the role that the cloud of the free carriers (FC) and free excitons (FE) around the drop plays in the drop recombination, and to the influence of the deformation potential on the evaporation of the excitons from the drop.

We have investigated the thermodynamic spatial, and kinetic characteristics of a quasi-equilibrium EHD–FE–FC system in nonuniformly compressed Ge. This investigation included a study of the microwave conductivity and of the cyclotron resonance (CR) under conditions of pulsed laser excitation. Experience has shown that microwave methods are very productive in investigations of exciton condensation.[3–5] In particular, CR is an effective method of studying the FC and yields the total number of carriers (by measuring the line intensity) and their collision frequency (by measuring the line width). It is known that large EHD are produced in a nonuniformly elastically strained crystal, when the band structure is altered and a potential-energy maximum is produced inside the crystal. A consequence of the pressure gradient in the potential well is a spatial inhomogeneity of the distributions of the FC and FE located above the drop; this leads to singularities of the CR observed under these conditions. To analyze the experimental spectra, the known CR theory was modified to take into account the nonuniform distribution of the carriers and the distortion of the electromagnetic field in the microwave resonator by the drop. An analysis of the CR spectra within the framework of this theory has made it possible to determine the FC density and their collision frequency, and to obtain a picture of their distribution in the sample.

In addition, we investigated the kinetics of microwave absorption by FC in the absence of a magnetic field at various temperatures. The experimental results are discussed on the basis of an analysis of the kinetic equation for the EHD–FE–FC system. These investigations have led to the conclusion that the evaporation of the excitons from the drop influences the drop kinetics, and allowed us to determine a number of important thermodynamic parameters of the system, such as the condensation energy, the work function, and the exciton binding energy in the high-pressure limit.

2. EXPERIMENTAL TECHNIQUE

We investigated samples of dislocation-free n-Ge with residual impurity density $\sim 7 \times 10^{11}$ cm^{-3} (sample No. 1) and $\sim 5 \times 10^{12}$ cm^{-3} (sample No. 2), in the form of disks 4 mm in diameter and 2 mm thick. The compression was along the ⟨111⟩ and ⟨110⟩ axes using a kaprolon plastic screw of 1.8 mm diameter.

The experimental setup for the investigation of the cyclotron resonance consisted of a microwave CR video-spectrometer ($\lambda = 3.2$ cm) with a reflecting H_{102} cavity with $Q \sim 10^3$ and a Q-switched YAG:Nd^{3+} laser. The laser pulse duration was ~ 10 nsec, and the maximum pulse energy was $\sim 10^{-4}$ J, and $\lambda = 1.06$ μm. The receiving channel of the apparatus used to record the CR spectra consisted of a microwave detector, a broadband amplifier, a strobe-integrator, an automatic recorder, and an oscilloscope. The use of the strobing regime has made it possible to plot the CR spectra at different delays relative to the laser pulse. We investigated first the luminescence of the samples and deter-

 0038-5646/81/020322-07$02.40

mined the pressure from the position of the maximum of the EHD emission line,[6] and the lifetime of the EHD from the radiation kinetics. The CR was then investigated without changing the compression conditions. The Ge crystal was placed at the maximum of the microwave-resonator electric field. The external magnetic field H was parallel to the sample surface and to the compression direction. The microwave conductivity was investigated with an analogous setup at $H = 0$.

3. EXPERIMENTAL RESULTS

a. Cyclotron resonance of free carriers under conditions of existence of a large drop

Uniaxial strains in germanium, depending on the applied pressure, lift partially or fully the degeneracy in the conduction and valence bands, and the CR spectra are altered as a result. The first investigations of CR in nonuniformly compressed Ge were performed by Markiewicz *et al.*,[2] who found that at an arbitrary orientation of the crystal relative to the external magnetic field, the spectrum has only one electron line and not the four lines of approximately equal intentisy observed in the absence of pressure. It was concluded therefore that most of the electrons in the cloud over the drop belong to one valley and are localized in the potential-well region where the EHD is located.

Figure 1 shows typical CR spectra of nonuniformly compressed Ge (sample No. 1) at $T = 4.2$, obtained with various delays relative to the laser pulse. The applied pressure was ~1500 bar. It is seen that the spectra have a complicated form: they have a narrow central line, a clearly pronounced broad right-hand wing, and a constant component independent of H. At relatively short delays ($t_d < 50$ μsec) the spectral lines are poorly resolved, and the shape of the spectrum points to the presence of strongly broadened FC spectral lines typical of undeformed Ge (inset of Fig. 1). At long delay times, the CR spectra have each a single asymmetric line with a maximum corresponding to an electron effective mass $m^* = 0.08\ m_0$. In the interval $t_d = 50$–1000 μsec, identical line shaped were obtained with little variation in the amplitude. At larger $t_d > 1000$ μsec the right-hand line wing and the dc component decrease gradually. This is clearly seen in Fig. 2, where the amplitude-normalized CR spectra corresponding to different delays are compared.

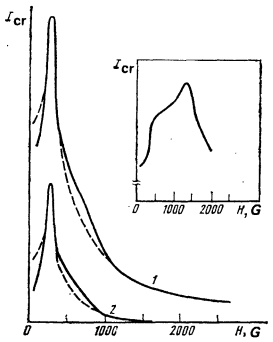

FIG. 1. CR spectra of nonuniformly deformed Ge at various delays after the laser pulse: 1) $t_d = 1850$ μsec, 2) $t_d = 2400$ μsec. The maximum corresponds to an electron effective mass $m^* = 0.08\ m_0$. Dashed—computer calculation of the CR line shape by formula (22). Inset—spectrum with 10 μsec delay; the second maximum corresponds to a heavy-hole effective mass $m^* = 0.39\ m_0$. Sample No. 1, $T = 4.2$ K, $p \approx 1500$ bar, $p \parallel \langle 111 \rangle \parallel H \perp E$. Initial excitation level ~ 10^{13} electron-hole pairs in sample, characteristic lifetime $\tau_0 \approx 500$ μsec.

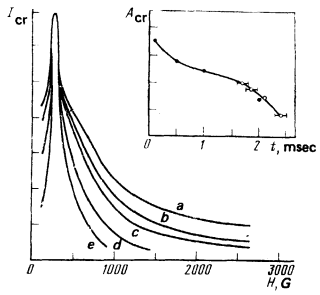

FIG. 2. CR spectra normalized in amplitude at various delays relative to the laser pulse. Curve *a* corresponds to delays 100, 500, and 1000 μsec; *b*) 1700 μsec; *c*) 1850 μsec; *d*) 2100 μsec; *e*) 2400 μsec. Inset—amplitude of CR line ($m^* = 0.08\ m_0$) vs. the delay for the spectra shown in Figs. 1 and 2. The light and dark circles correspond to different experiments. The relative error in the time fit of the experiments is indicated.

We have assumed that the observed singularities in the spectrum are due to the inhomogeneity of the FC density around the drop. The narrow line obviously belongs to peripheral regions with relatively low carrier density and collision frequency ν, while the broad wing belongs to the surface layers directly adjacent to the drop, where the density n_{es} and ν are maximal. There are no lines corresponding to other effective masses. The inset of Fig. 2 shows the dependence the CR line amplitude on the delay time. Similar results were obtained with sample No. 2 at two pressures, ~600 and 1000 bar. All the characteristic relations are the same for both samples.

b. Kinetics of microwave conductivity

We investigated the pulsed microwave conductivity[1)] in nonuniformly deformed Ge at various temperatures and optical-excitation levels. Figure 3 shows a series

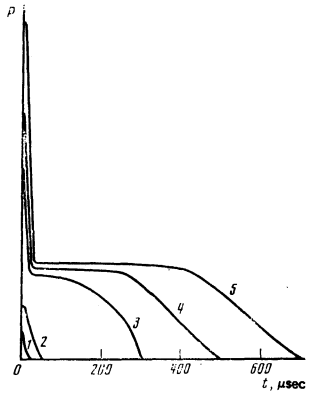

FIG. 3. Kinetics of microwave absorption signal of nonuniformly deformed Ge at various optical-excitation levels corresponding to the numbers of the generated electron hole pairs in the sample: 1) 10^{10}; 2) 3.5×10^{10}, 3) 3×10^{11}, 4) 5×10^{11}. Sample No. 2, $T = 4.2$ K, $p \parallel \langle 111 \rangle$, $p \approx 1000$ bar, $\tau_0 \approx 200$ μsec.

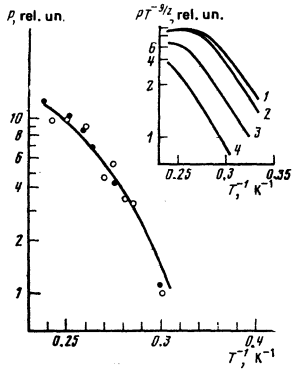

FIG. 4. Dependence of amplitude of the plateau section of the microwave absorption spectrum on the temperature, $p \parallel \langle 111 \rangle$. o) sample No. 2, $p \approx 1500$ bar; •) sample No. 2; solid curve —calculation of microwave absorption by formula (20) for $E_w = 4.6$ meV and $n_{es} = 3.5 \times 10^{12}$ cm^{-3}. Inset—calculated $P(T)$ dependences for: 1) $E_w = 4.6$ meV, $n_{es} = 4 \times 10^{12}$ cm^{-3}; 2) $E_w = 4.8$ meV, $n_{es} = 4 \times 10^{12}$ cm^{-3}; 3) $E_w = 4.6$ meV, $n_{es} = 2 \times 10^{12}$ cm^{-3}; 4) $E_w = 4.6$ meV, $n_{es} = 10^{12}$ cm^{-3}.

of signals obtained at $T = 4.2$ K and corresponding to different laser-pulse energy levels. At low levels (curves 1 and 2) the signal duration is approximately 10 μsec.

Starting with the second excitation level, the microwave conductivity signal is abruptly changed: the signal duration increases by 1–2 orders, and a plateau section appears with an amplitude that varies little with excitation intensity. At high pump levels, the signal duration increases all the way to the millisecond range.

As shown in Ref. 7, the microwave conductivity signal in nonuniformly compressed Ge at $T \gtrsim 3$ K is due to free carriers that are at equilibrium with the exciton gas in the EHD. The observed evolution of the signal shape with changing excitation level is attributed to the fact that in the case of weak excitation (below the EHD production threshold) the FC kinetics is connected with the rather rapid decay of the excitons (this corresponds to curves 1 and 2 of Fig. 3), whereas under strong excitation it reflects the EHD kinetics, since the source of the FC under these conditions are the excitons evaporated from the EHD.

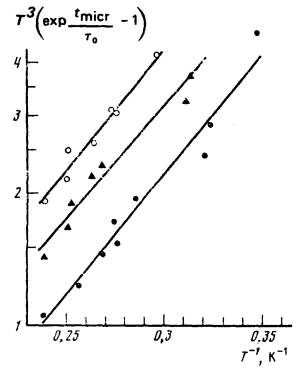

FIG. 5. Microwave absorption pulse duration t_{micr} vs. temperature: •) sample No. 2, $p_1 \parallel \langle 110 \rangle$; ▲) sample No. 2, $p_2 \parallel \langle 111 \rangle$; o) sample No. 1, $p_3 \parallel \langle 111 \rangle$. Solid lines—calculation by formula (24) at $\Phi = 1.1 \pm 0.1$ meV.

When the temperature drops to < 4.2 K the amplitude of the plateau section (P) decreases and the duration (t_{micr}) increases. Figures 4 and 5 show the experimental plots of $P(T)$ and $t_{micr}(T)$.

4. THEORY

In this section we analyze the CR spectra and the microwave-conductivity kinetics of nonuniformly deformed germanium.

a. Kinetic equations for the large EHD-FE-FC system

We consider the kinetics of this system in Ge under conditions of nonuniform crystal deformation. The change of the potential energy of the FC in the potential well can be approximated by the parabola

$$E_s = -E_s^0 + \alpha r^2, \tag{1}$$

where E_S^0 is the shift of the forbidden band due to the crystal deformation, α is the pressure parameter (~10 meV/mm^2, Ref. 2), and r is the distance to the center of the well. Then, assuming a Boltzmann spatial distribution of the FC over the drop surface, we express $n_e(r)$ in the form

$$n_e(r) = n_{es} \exp[-\alpha(r^2 - R^2)/kT], \tag{2}$$

where n_{es} is the FC density near the drop surface at $r = R$. The total number of carriers around the drop is given by the integral

$$N_e(R) = 4\pi \int_R^\infty n_{es} \exp[-\alpha(r^2 - R^2)/kT] r^2 dr = 2\pi n_{es} (kT/\alpha)^{3/2} \exp(\alpha R^2/kT) \times \{(\alpha/kT)^{1/2} R \exp(-\alpha R^2/kT) + \tfrac{1}{2}\pi^{1/2}[1 - \operatorname{erf}(\alpha/kT)^{1/2} R]\}, \tag{3}$$

where

$$1 - \operatorname{erf} z = \int_z^\infty e^{-x^2} dx.$$

Figure 6 shows the dependence, calculated by formula (3), of the number of the FC in the gas phase on the relative drop radius. At $R < R_c = (kT/\alpha)^{1/2} \approx 200$ μm we have

$$N_e(R) \approx n_{es} (\pi kT/\alpha)^{3/2}. \tag{4}$$

The quantity $(\pi kT/\alpha)^{3/2} = V$ has the meaning of the effec-

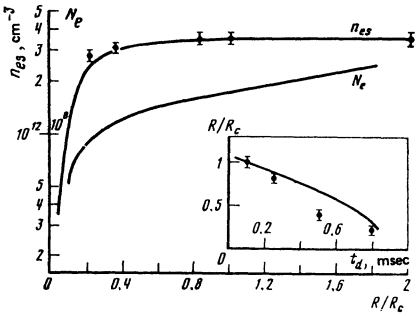

FIG. 6. Dependence of FC density at the EHD surface (n_{es}) and of the total number of carriers in the cloud (N_e) on the relative radius (R/R_c): points— from the reduction of the CR spectra, solid curves—from the solution of the kinetic equations (10) and from formula (3). Inset—plot of R/R_c against t_d, calculated from formula (12). Points—dependence of R/R_c on t_d from the results of the reduction of the CR spectra.

tive volume in the FC and FE gas phase. Similar relations can be written for the number of the FE:

$$N(R)\approx n_s(\pi kT/\alpha)^{3/2}. \quad (5)$$

At $R>200$ μm it follows from (3) that $N_e(R)\propto R$.

We now write down the kinetic equations for all three components of the EHD–FC–FE system. Owing to the spatial inhomogeneity of the gas-phase particle distributions, it is convenient to write the equations for the total number of the FC (N_e), of the FE (N), and the number of electron-hole pairs in the condensed phase (N_0):

$$dN_e/dt=-N_e/\tau_e+4\pi R^2 v_{eT}(n_{eT}-n_e)+S-S_e, \quad (6)$$
$$dN/dt=-N/\tau+4\pi R^2 v_T(n_T-n)+S_e-S, \quad (7)$$
$$dN_0/dt=-N_0/\tau_0-4\pi R^2 v_T(n_T-n), \quad (8)$$

where the first terms in the right-hand sides describe the recombinations of the FC, FE, and EHD proper, the second describe their evaporation and their flow back to the drop, and the terms $S_e=\int_V \beta n_e^2(r)dV$ and $S=\int_V \gamma n(r)dV$ describe the binding of the FC into excitons and the thermal dissociation of the FE; β and γ are the coefficients of the corresponding processes; τ_0 is the EHD lifetime; τ_e, τ, n_{eT}, and n_T are the lifetimes and thermodynamic concentrations of the FC and FE; v_{eT} and v_T are their thermal velocities; the integration is over the volume of the potential well.

The quasistationary solutions of Eqs. (6) and (7), neglecting the small terms S_e and S and taking (4) and (5) into account, are of the form

$$n_{es}=n_{eT}\frac{R^2}{R^2+(\pi kT/\alpha)^{3/2}/4\pi v_{eT}\tau_e}, \quad (9)$$

$$n_s=n_T\frac{R^2}{R^2+(\pi kT/\alpha)^{3/2}/4\pi v_T\tau}, \quad (10)$$

from which it follows that up to the time that the drop reaches a sufficiently small radius the concentration of the gas-phase particles next to the drop surface is maintained at thermodynamic equilibrium (see Fig. 6). Inasmuch as $T\approx 4$ K the FE density greatly exceeds the FC density, we shall use for the description of the drop kinetics the equations (7) and (8), neglecting evaporation and the return flow of the FC compared with the analogous processes for the excitons. In the quasistationary approximation ($dN/dt=0$), taking (5) into account, we get

$$\ln\left(\frac{R^3+q}{R_0^3+q}\right)=-\frac{t}{\tau_0}, \quad (11)$$

where $q=3\tau_0 N/4\pi n_0\tau$, n_0 is the particle density in the EHD, and $R_0=R$ at $t=0$; it follows therefore that

$$R(t)=[(R_0^3+q)\exp(-t/\tau_0)-q]^{1/3}. \quad (12)$$

Assuming that $R(t)=0$ at $t=t_{EHD}$ we get from (12)

$$t_{EHD}=\tau_0\ln(1+R_0^3/q). \quad (13)$$

The quantity t_{EHD} has a strong temperature dependence, since $q\propto(\pi kT/\alpha)^{3/2}n_s$, and according to (10)

$$n_s\approx n_T=g(m^*kT/2\pi\hbar^2)^{3/2}\exp(-\Phi/kT), \quad (14)$$

where Φ is the condensation energy; $m^*=0.41m_0$; $g=4$ in Ge in the high-pressure limit.

It is seen from (13) that when the temperature is lowered the value of q decreases rapidly, and this causes t_{EHD} to increase. The experimental $t_{EHD}(T)$ relation makes it obviously possible to determine Φ.

b. Microwave conductivity and cyclotron resonance in nonuniformly deformed Ge

For a more rigorous justification of the qualitative interpretation proposed above for the form of the CR spectra, as well as to obtain quantitative information on the FC, we carried out a computer reduction of the spectra on the basis of a model which, in contrast to the theory of CR in the homogeneous case,[9] required that the specific features of the spatial inhomogeneity of the problem be taken into account, namely; the Boltzmann distribution of the FC density in the potential well around the EHD, the coordinate dependence of the FC collision frequency, whose value is determined at sufficiently high FC density by the electron-hole and electron-exciton collisions,[10] as well as distortions of the electric field in the microwave resonator near the surface of a large EHD.

In the present section we calculate the microwave absorption and the CR line for FC in the presence of an EHD, with account taken of the aforementioned factors and of the results of the solution of the kinetic equations. The average power absorbed by the FC in the microwave field is described by the formula[11]

$$P=\frac{E_i^2e^2}{m^*}\frac{n_e\nu}{\omega^2(1-\omega_p^2/\omega^2)^2+\nu^2}, \quad (15)$$

where $E_i=E_0/[1+\varkappa(\varepsilon_0-1)]$ is the electric microwave field inside the sample; E_0 is the external microwave field; $\omega_p=(4\pi n_e e^2/m^*\varepsilon_0)^{1/2}$ is the FC plasma frequency, ε_0 is the dielectric constant of Ge; $\varkappa$ is the depolarizing factor; n_e, m^*, and ν are the density, effective mass, and the collision frequency of the FC; ω is the frequency of the microwave generator.

At sufficiently high density of the gas phase (FC and FE), ν is determined by collisions with phonons as well as with carriers and excitons. We can therefore write $\nu=\nu_{ph}+bn_e+cn$, where ν_{ph} is the frequency of the electron-phonon collisions, and b and c are coefficients. Taking into account the identity of the spatial distributions of the FC and FE in the potential well, as determined by relation (2), we can express $\nu(r)$ in the form

$$\nu(r)=\nu_{ph}+(\nu_{e-h}^s+\nu_{e-ex}^s)\exp[-\alpha(r^2-R^2)/kT], \quad (16)$$

where ν_{e-h}^s and ν_{e-ex}^s are the electron-hole and electron-exciton collision frequencies near the EHD surface. We note that the dependence of ν on the FC density was investigated earlier in Ref. 10 for the case of small drops in Ge at $T=4.2$ K.

The change of the microwave field near a large EHD can be approximately regarded as distortion by a metallic sphere. A similar problem for a sphere in a microwave resonator was considered in Ref. 12. Assuming the skin layer of a large EHD to be $\delta\approx 10$ μm thick,[13] using the solution obtained in Ref. 12 in the approximation $R/\delta\gg 1$, and averaging over the angles we obtain the following value of the microwave field outside the drop:

$$E_0(r)=E^*[1+2(R/r)^3+3(R/r)^6]^{1/2}, \quad (17)$$

where E^* is the field in the absence of the metallic sphere. To calculate the cyclotron absorption we need the field alues parallel and perpendicular to the external magnetic field **H**:

$$E_{0\perp}(r)=E^*[1+2(R/r)^3+1{,}8(R/r)^6]^{1/2}, \quad (18)$$

$$E_{0\parallel}(r)=E^*[1{,}2(R/r)^6]^{1/2}. \quad (19)$$

Now, using (12) and (15)–(17), we can find the microwave absorption in the FC cloud over the drop in a zero magnetic field in the form of the following integral:

$$P=\frac{4\pi e^2}{[1+\varkappa(\varepsilon_0-1)]^2 m^*}\int_R^\infty \frac{E_0^2(r)n_e(r)\nu(r)}{\omega^2[1-\omega_p^2/\omega^2]^2+\nu^2(r)}r^2dr. \quad (20)$$

The active conductivity of the sample in the magnetic field (with allowance for the plasma shift) is described by the relation[9]

$$\sigma'(H)=\frac{n_e e^2}{m^*\nu}\frac{1+\omega_0^2/\nu^2+\omega_c^2/\nu^2}{(1+\omega_c^2/\nu^2-\omega_0^2/\nu^2)^2+4\omega_0^2/\nu^2}, \quad (21)$$

where $\omega_0=eH/m^*c$ is the cyclotron frequency, c is the speed of light, $\omega_0=[1-(\omega_p/\omega)^2]$, and ω_p is the plasma frequency.

It follows from (19) that the presence of a large EHD in the microwave resonator leads to the appearance of an electric field component $E_{0\parallel}$ parallel to the external magnetic field. The calculate the line shape it is therefore necessary to take the longitudinal conductivity into account. Then, taking into consideration (2), (16), (18), (19), and (21), the total cyclotron absorption outside the large EHD is described by the integral

$$P(H)=\frac{4\pi e^2}{[1+\varkappa(\varepsilon_0-1)]^2 m^*}\int_R^\infty \frac{E_{0\perp}^2(r)n_e(r)[1+\omega_0^2/\nu^2+\omega_c^2/\nu^2]}{\nu[1+\omega_c^2/\nu^2-\omega_0^2/\nu^2]^2+4\omega_0^2/\nu^2}r^2dr$$

$$+\frac{4\pi e^2}{[1+\varkappa(\varepsilon_0-1)]^2 m^*}\int_R^\infty \frac{E_{0\parallel}^2(r)n_e(r)\nu r^2dr}{\omega^2[1-\omega_p^2/\omega^2]^2+\nu^2}. \quad (22)$$

5. ANALYSIS OF EXPERIMENTAL RESULTS

The CR line shape was calculated from Eq. (22) with a computer. By comparing the experimental and calculated spectra, with the three parameters $\nu_s=\nu(R)$, n_{es}, and R/R_c varied, we were able to determine a number of important characteristics of the gas phase. Figure 1 shows a comparison of the calculated and experimental spectra. The independence of the CR line shape of t_d in the interval 0.1–1 msec (curve a of Fig. 2) has allowed us to conclude that it does not depend on the drop radius. We therefore assumed $R/R_c=2$ in the calculation of the spectrum at $t_d=0.5$ msec, and varied the quantities n_{es} and ν_s [we note that if we use the experimental estimates $\alpha=7$ meV/mm^2 (Ref. 14) and $\alpha=11$ meV/mm^2 (Ref. 2), then $R_c\approx 200$ μm]. A satisfactory agreement of the observed spectrum with the calculated one was obtained at $n_{es}=(3.5\mp 0.3)\times 10^{12}$ cm^{-3} and $(\nu_s=3.5\mp 0.5)\times 10^{11}$ sec^{-1}. Next, using these values, we varied R/R_c in the calculation in the range 1.4–2.5. The shape of the spectrum remained practically unchanged, in good agreement with experiment. The values of n_{es} and ν_s obtained above where subsequently used to reduce the CR spectra, whose forms were now dependent on t_d and consequently also on R (Fig. 1 and curves b–e of Fig. 2). In this case we varied the quantities R/R_c and n_{es}, and the change of ν_s was assumed, obviously, to be proportional to n_{es}. Good agreement between the observed and calculated spectra was obtained at $n_{es}=(3.5\pm 0.3)\times 10^{12}$ cm^{-3} and $R/R_c=1.0$ for $t_d=1700$ μsec, $n_{es}=(3.2\pm 0.3)\times 10^{12}$ cm^{-3} and $R/R_c=0.83\pm 0.05$ for $t_d=1850$ μsec, $n_{es}=(3.2\pm 0.3)\times 10^{12}$ cm^{-3} and $R/R_c=0.4\pm 0.05$ for $t_d=3100$ μsec, and $n_{es}=(2.8\pm 0.3)\times 10^{12}$ cm^{-3} and $R/R_c=0.22\pm 0.05$ for $t_d=2400$ μsec.

The indicated values of the FC densities and of the values of R/R_c corresponding to them are shown in Fig. 6 together with the theoretical n_{es} (R/R_c) relation, which is the solution of the kinetic equations (10). It is seen that, with sufficiently good agreement, both the experimental and the calculated data allow us to conclude that a noticeable degrease of n_{es} begins at $R/R_c\approx 0.3$. or $R\approx 60$ μm. In addition, the presented values of R/R_c obtained by reducing CR spectra with different delays t_d yield information on the kinetics of the drop. The inset of Fig. 6 shows the data on the time dependence of R/R_c, which are compared with the solution of the kinetic equation for the drop radius given by Eq. (12).

The spectra contain two sections in which deviations from the calculated curves are obtained, namely at the initial and central parts (Fig. 1). The first of the discrepancies is possibly due to the parabolicity of the function $E_S(r)$ at large R, which can take place when the drop dimensions are comparable with those of the potential well. As for the second section, it constitutes a group of unresolved hole lines corresponding to transitions between Landau levels that are typical of Ge compressed in the ⟨111⟩ direction[15] and are additionally smeared because of the nonuniform carrier density. The character of the spectrum at short delays (see the inset of Fig. 1) indicates that during the first ~50 μsec after the laser pulse a sufficient number of FC are in the low-pressure region in which, apparently, small drops still exist.

The results allow us to conclude that the FC are spatially distributed in the sample in the presence of a large EHD. The presence in the CR spectra of single electron lines with orientations along ⟨111⟩ $\|\mathbf{H}$ indicates that all the electrons belong to a single valley and is evidence that the carriers in the sample are located near the drop. The satisfactory description of the shape of the spectrum with the aid of the indicated model confirms the validity of expression (1), from which we can obtain the effective size of the cloud (the distance over which the carrier density decreases by a factor of e): $\delta r\approx 60$ μm at $R\approx 400$ μm.

We discuss now the results on microwave absorption in the absence of a magnetic field. As shown in Ref. 11, at low FC densities the microwave-absorption signal is proportional to the total number of FC in the sample, given in our case by Eq. (3) where, as follows from the solutions of the kinetic equations (9), $n_{es}\approx n_T$, the latter being the thermodynamic equilibrium value of the FC density. It is known that

$$n_{eT}=g(m^*kT/2\pi\hbar^2)^{3/2}\exp(-E_w/2kT), \quad (23)$$

where g is the degeneracy factor and E_w is the work function. Thus, in the case of low densities the amplitude of the microwave-absorption signal is $P\propto T^{3/2}$

$\times \exp(-E_w/2kT)$, so that the $P(T)$ relation can be used to determine E_w.

In spatially inhomogeneous case, $P(T)$ is described by the integral of (20), where account is taken also of the temperature dependences of ν and of the effective volume of the FC cloud.

To obtain from the experimental temperature dependence of the microwave-absorption temperature the value of the work function of the FC from EHD, the integral of (20) was calculated with a computer for different temperatures, with E_w, n_{es}, and R varied (see Fig. 4). A comparison of the calculated and experimental $P(T)$ yields $E_w = 4.6 \pm 0.2$ meV and $n_{es} = 3.5 \times 10^{12}$ cm^{-3} at all values $R < 300$ μm. We note that a like value of E_w was obtained in Ref. 7 for the ⟨110⟩ compression direction.

We turn now to the temperature dependence of the microwave-conductivity signal duration. Since the proper lifetime of the FC is ~10^{-7} sec,[4] it is natural to identify the signal duration ~10^{-3} sec with the total lifetime of the large EHD, which is the source that maintains the number of the FC in equilibrium for a long time. Starting from this assumption ($t_{EHD} = t_{micr}$), we have determined the condensation energy from the experimental $t_{micr}(T)$ relation, by transforming (13) and (14) into

$$\frac{\Phi}{kT} = \ln\left[T^{3}\left(\exp\frac{t_{micr}(T)}{\tau_0} - 1\right)\right] + \text{const.} \qquad (24)$$

A least-squares reduction of the right-hand side of (20) as a function of $1/T$ yielded for the FE an energy that is equal, within the limits of error, for the two different directions, namely $\Phi = 1.1 \pm 0.1$ meV (Fig. 5). We note that the increase of t_{micr} with decreasing T means physically that the lifetime of the drop is longer at low temperature, because of the lower rate of exciton evaporation.

A close value, $\Phi = 1$ meV, was obtained in Ref. 16 in the limit of a strong uniform pressure, where there is obviously no drawing of the excitons by the potential well. Thus, the hypothesis advanced in Ref. 2 and attributing the weak temperature dependence of the lifetime of a large EHD to this effect is apparently incorrect, and the experimental result is more readily due only to the relatively small share of the evaporation compared with the intrinsic recombination of the drop. The sensitive microwave-conductivity technique nevertheless reveals clearly the exciton evaporation effect and makes it possible to determine Φ.

The results obtained directly from the reduction of the experimental data yield additional information of the system, if certain simple relations are used. In fact, the condensation energy Φ and the thermodynamic equilibrium density of the FE (n_T) are connected by formula (14), from which it follows that $n_T = 10^{15}$ cm^{-3} at $\Phi = 1.1$ meV. We note that this value of n_T is somewhat lower than in undeformed Ge, where Φ is noticeably larger. The reason is the lifting of the degeneracy in uniaxial deformation.

Under conditions of thermodynamic equilibrium in the gas phase, the following relation hold between the FE and FC densities[17]:

$$n_{eT} = n_T^{1/2}(m^* kT/2\pi\hbar^2)^{3/4}\exp(-\mathscr{E}_0/kT), \qquad (25)$$

where $m^* = 0.047\, m_0$ and $\mathscr{E}_0$ is the exciton binding energy. Taking the values of n_{eT} and n_T determined above into account, we obtain the exciton binding energy $\mathscr{E}_0 = 3.5 \pm 0.2$ meV. This is a substantially more accurate value of $\mathscr{E}_0$ than previously obtained.[16]

Using the thermodynamic carrier density $n_{eT} = 3.5 \times 10^{12}$ cm^{-3} obtained in the reduction of the CR spectra, we can find from (23) the work function E_w of the FC from a large EHD, calculated to be 4.6 meV. As shown above, analysis of the temperature dependence of the microwave absorption amplitude yields the same value. The good agreement between values of E_w measured by independent methods attests to the correctness of the interpretation proposed in this article for the experimentally observed regularities.

The rather large amount of data obtained by analyzing the CR spectra and the microwave-absorption kinetics in a zero magnetic field, concerning the thermodynamic, kinetic, and spatial characteristics of the EHD–FE–FC system in inhomogeneously deformed Ge, is evidence of the abundant information that the microwave methods can provide in the investigation of exciton condensation.

The authors thank L. V. Keldysh, V. A. Milyaev, V. A. Sanina, and S. G. Tikhodeev for a discussion of the work.

[1)]The quantity recorded in the experiment was the active component of the complex microwave conductivity, i.e., the microwave absorption.

[1]R. S. Markiewicz, J. P. Wolfe, and C. D. Jeffries, Phys. Rev. Lett. 32, 1357 (1974).
[2]R. S. Markiewicz, J. P. Wolfe, S. M. Kelso, J. E. Furneax, and C. D. Jeffries, Phys. Rev. B18, 1479 (1978).
[3]J. C. Hensel, T. G. Phillips, and T. M. Rice, Phys. Rev. Lett. 30, 227 (1973).
[4]Trudy FIAN, vol. 100, M., Nauka, 1977.
[5]A. G. Makarov, A. A. Manenkov, G. N. Mikhaĭlova, and A. S. Seferov, Pis'ma Zh. Eksp. Teor. Fiz. 31, 440 (1980) [JETP Lett. 31, 385 (1980)].
[6]C. Benoit a la Guillaume, M. Voos, and F. Salvan, Phys. Rev. B5, 3079 (1972).
[7]A. A. Manekov, V. A. Milyaev, G. N. Mikahĭlova, and A. S. Seferov, Pis'ma Zh. Eksp. Teor. Fiz. 24, 141 (1976) [JETP Lett. 24, 122 (1976)].
[8]R. S. Markiewich, J. P. Wolfe, and C. D. Jeffries, Phys. Rev. B15, 1988 (1977).
[9]G. Dresselhaus, A. F. Kip, and C. Kittel, Phys. Rev. 98, 368 (1955).
[10]A. A. Manenkov, V. A. Milyaev, and V. A. Sanina, Dokl. Akad. Nauk SSSR 250, 1371 (1980) [Sov. Phys. Dokl. 25, 116 (1980)].
[11]B. V. Zubov, A. A. Manenkov, V. A. Milyaev, G. N. Mikhaĭlova, T. M. Murina, and A. S. Seferov, Fiz. Tverd. Tela (Leningrad) 18, 706 (1976) [Sov. Phys. Solid State 18, 406 (1976)].
[12]M. A. Divil'kovskiĭ, Zh. Tekh. Fiz. 9, 433 (1939).
[13]A. S. Kaminskiĭ, Ya. E. Pokrovskiĭ, and A. E. Zhidkov, Zh. Eksp. Teor. Fiz. 72, 1962 (1977) [Sov. Phys. JETP 45, 1030 (1977)].
[14]A. G. Makarov, A. A. Manenkov, G. N. Mikhaĭlova, and

A. S. Seferov, Pis'ma Zh. Eksp. Teor. Fiz. 30, 411 (1979) [JETP Lett. 30, 385 (1979)].
[15]J. C. Hensel, Sol. Ste. Commun. 4, 231 (1966).
[16]B. J. Feldman, H. -h. Chou, and G. K. Wong, Sol. St. Commun. 26, 209 (1978).
[17]Z. A. Insepov, T. E. Norman, and L. Yu. Shruova, Zh. Eksp. Teor. Fiz. 71, 1960 (1976) [Sov. Phys. JETP 44, 1028 (1976)].

Translated by J. G. Adashko

Extended description of a solution of linear polymers based on a polymer-magnet analogy

E. S. Nikomarov and S. P. Obukhov

L. D. Landau Institute of Theoretical Physics, Academy of Sciences of the USSR
(Submitted 1 July 1980)
Zh. Éksp. Teor. Fiz. **80**, 650–665 (February 1981)

It is shown that the problem of the behavior of a long polymer molecule in a solution of other linear polymers can be reduced to the problem of the correlation functions of an anisotropic magnet. Expressions are obtained for the correlation function of the ends of a probe molecule. The condition for globule formation, the mean size of the polymer coil, etc., are also determined. The case when the polymers are adsorbed on a surface (two-dimensional polymer solution) is considered separately. It is shown that in this case the familiar results obtained for two-dimensional magnets can be employed. Other problems are mentioned in which the analogy between a polymer solution and a magnet can be applied.

PACS numbers: 36.20. – r, 82.35. + t

1. INTRODUCTION

The analogy between a solution of linear polymers and a magnet with zero number of components (first established by des Cloizeaux)[1] makes it possible to relate the average parameters for the given solution to the thermodynamic averages of the zero-component Heisenberg model. Des Cloizeaux used this analogy to determine the scaling relationships between the parameters characterizing a strongly fluctuating polymer solution, and connected them with the already familiar scaling relationships for a magnet near the phase-transition point. The state of the magnet is unambiguously given by two parameters—the temperature and the magnetic field—in terms of which we may express all the remaining correlation radii of the longitudinal and transverse fluctuations, the free energy, etc. In exactly the same way, given any two parameters which characterize the polymer solution—say, the monomer density and the average degree of polymerization—we may determine the correlation radius in solution, the average separation between ends of the polymer, and the entropy. Here, within the framework of the "polymer solution–magnet" analogy, we cannot obtain in principle more detailed characteristics of the solution—the equilibrium polymer length distribution, the average separation between ends of a polymer of a given length—let alone obtain an expression for the correlation function of a polymer placed into the given solution and having other chemical and physical properties.

In this work, we present a method which allows us to obtain all these detailed characteristics: the probe molecule method. We consider a magnet composed of two interacting subsystems; using one subsystem we will describe the polymer solution, and using the other subsystem we will describe an isolated polymer molecule in this solution. We find that the problem is reduced to calculation of the correlation functions of an anisotropic magnet with double the number of components—a well-known simple problem.[2] The polymer–magnet analogy is used in our work not only in the region of strongly fluctuating solutions of linear polymers, but also to describe concentrated solutions (melts) and solutions containing cyclic polymers. The results obtained for melts agree with the familiar results[3] obtained by ordinary perturbation theory methods. The case of a two-dimensional solution of polymers (polymers which are adsorbed on a surface) is an exception for which perturbation theory is not applicable. In this case, the polymer–magnet analogy makes it possible to use the results obtained by Polyakov for two-dimensional magnets with an arbitrary number of components to describe the polymer solution.

2. HEISENBERG MODEL IN THE LIMITING CASE $n \to 0$. CORRESPONDENCE BETWEEN A MAGNET AND A POLYMER

Let us consider a lattice[1)] with classical n-component spins of length $n^{1/2}$ at the lattice points. We write the spin interaction Hamiltonian as

$$H = -\sum_{i,k,\alpha} J_{ik} S_\alpha(\mathbf{x}_i) S_\alpha(\mathbf{x}_k) - \sum_i h_1(\mathbf{x}_i) S_1(\mathbf{x}_i). \qquad (2.1)$$

Here $J_{ik} = J(\mathbf{x}_i - \mathbf{x}_k)$ is the interaction parameter between spins located at the lattice points i and k; the index α takes on values from 1 to n; h is the external magnetic field, directed along the 1 axis. The summation is over all the lattice points.

 0038-5646/81/020328-08$02.40